# Adsorption removal of arsine by modified activated carbon

**Ming Jiang · Yangwei Bai · Ping Ning ·
Xiaofeng Huang · Hongpan Liu · Jianqiu Fu**

**Abstract** The modified activated carbon adsorbents were prepared by impregnation method for removal of arsine ($AsH_3$). The results show that the activated carbons modified with sulfonated cobalt phthalocyanine (CoPcS) and $Cu(NO_3)_2$ (denoted as Co/Cu) is found to have significantly enhanced adsorption removal ability. The effects of CoPcS content, calcination temperature, $O_2$ content and pore structure on the $AsH_3$ adsorption are investigated. The optimum conditions for removal of $AsH_3$ are 0.02 wt% of CoPcS content, 400 °C of calcination temperature and 4 vol% of $O_2$ content, respectively. The regions of micropores (14.7 Å < pore width < 20 Å) and mesopores (20 Å < pore width < 43.4 Å) play the predominant role for adsorbing $AsH_3$. The regeneration efficiency of deactivated Co/Cu/AC adsorbent is up to 71.2 %.

**Keywords** Arsine · Modified activated carbon · Adsorption · Sulfonated cobalt phthalocyanine

M. Jiang
College of Resources and Environment, Yunnan Agricultural University, Kunming 650201, China

M. Jiang · Y. Bai · P. Ning (✉) · X. Huang · H. Liu · J. Fu
Faculty of Environmental Science and Engineering, Kunming University of Science and Technology, Kunming 650500, China
e-mail: ningping58@126.com

Y. Bai
Chinese Research Academy of Environmental Sciences, Beijing 100012, China

## 1 Introduction

Arsine ($AsH_3$) as by-product is formed when arsenic-containing metals react with acids or during refining of arsenic-containing coal and ores (e.g., phosphate, copper and lead-zinc ores) (Ivandini et al. 2010; Trembly et al. 2007; Wang et al. 2011b). $AsH_3$ is an important process gas and a dopant used in the semiconductor industry for GaAs crystal growth (Ohno et al. 2003a, b; Oyama et al. 2000, 2003; Kawano et al. 2012), plasma immersion ion implantation (Yang et al. 2002), chemical beam epitaxy (CBE) (Hidaka et al. 1997) and metal organic chemical vapor deposition (MOCVD) (Cossel et al. 2010) processes. The toxicity of $AsH_3$ is about 7 times hihger than Lewisite (Goldman and Dacre 1989). When $AsH_3$ is inhaled, it may lead to lung, respiratory tract, bronchus, kidney serious damage and even death. Therefore, many countries strictly limit the concentration of $AsH_3$ in workshop. For example, the American Committee of government in Health and the Ministry of Environmental Protection of the People's Republic of China suggest that the permissible exposure limits of $AsH_3$ should be 0.016 mg/m$^3$ (Suh et al. 2009) and 0.001 mg/m$^3$, respectively. Furthermore, with the development of C1 (one carbon) chemical technology, synthesis gas (syngas) can be used to produce C1 chemical products such as methanol ($CH_3OH$), methanoic acid (HCOOH), etc. However, one of the most important factors of synthesis catalyst poisoning is the existence of low concentration $AsH_3$ in synthesis gas (Quinn et al. 2006; Quinn and Toseland 2008). Hence, it is of profound significance to remove $AsH_3$.

The main methods developed for removing $AsH_3$ from air and off-gas contain chemical absorption, catalytic decomposition, combustion, adsorption, etc. In recent years, the research attentions have been focused on the gas-solid adsorption of $AsH_3$ because of two main reasons. On

the one hand, the concentration of AsH₃ in air or off-gas is lower than other gaseous contaminants such as H₂S, PH₃, COS and so on (Wang et al. 2011b; Yuan et al. 2014). AsH₃ can be removed to very low concentration (less than permissible exposure limits of AsH₃) by selective adsorption. On the other hand, the various low-cost adsorbents for removing AsH₃ derived from different sources, and most of them had good regeneration property. Some of the reported adsorbents for removing AsH₃ from off-gas or synthesis gas include metal or metal oxide modified carbon (Quinn et al. 2006), activated carbon (AC) (Quinn et al. 2006), metal modified $\gamma$-Al₂O₃ (Rupp et al. 2013), metal-based alloy (Han et al. 2010), and metal loaded SBA-16 mesoporous molecular sieve (Howard et al. 2013).

The objective of this wok is to prepare modified activated carbon (AC) adsorbents for removing low concentration AsH₃ from a gas stream. The effects of sulfonated cobalt phthalocyanine (CoPcS) content, types of modifiers, calcination temperature, and inlet O₂ content on the AsH₃ adsorption removal were studied via the AsH₃ removal efficiency curve. The pore structure properties of the Co/Cu/AC adsorbents before and after AsH₃ adsorption were measured by N₂ adsorption/desorption experiments. The thermal regeneration of the spent Co/Cu/AC adsorbent was also explored.

## 2 Materials and methods

### 2.1 Adsorbent preparation

Commercial coal-based activated carbon (Changge, Henan, China) was used as the support in the experiments. The activated carbon (AC) particle size was $2 \pm 0.1$ mm. Sulfonated cobalt phthalocyanine (CoPcS) and Cu(NO₃)₂· 3H₂O were used as impregnation solutions. The AC was washed 5 times with distilled water at 60 °C, dried at 110 °C for 12 h. Then each AC samples ($10 \pm 0.1$ g) were impregnated with equal volume (50 mL) of CoPcS, Cu(NO₃)₂ or CoPcS/Cu solution at room temperature for 24 h, and dried at 110 °C for another 12 h, then calcined for 4 h. The samples were defined as Co/AC, Cu/AC, and Co/Cu/AC, respectively. The impregnation solution used to fabricate Co was prepared by dissolving CoPcS in anhydrous methanol solution. Cu was impregnated with an aqueous Cu(NO₃)₂ solution (0.2 mol/L), and Co/Cu was impregnated with the mixed solution consisting of a methanolic CoPcS solution and an aqueous Cu(NO₃)₂ solution (0.2 mol/L) at room temperature.

### 2.2 Adsorption of AsH₃

The AsH₃ adsorption process was conducted in a quartz adsorption column. The internal diameter and height of the adsorption column were 1.5 cm and 20 cm, respectively. The adsorption column was filled with 2 g of adsorbent. AsH₃ from gas cylinder was composed of 300 mg/m³ AsH₃ in N₂, which were mixed in a mixer with O₂ (99.999 % O₂) and introduced into the adsorption column under the flow rate of 350 ml/min at 60 °C. The model gas stream in adsorption column was heated by constant temperature water box. Figure 1 displays the schematic diagram of the adsorption experiment.

The AsH₃ concentration was measured by silver diethyldithiocarbamate spectrophotometric method. The AsH₃ concentration was measured every 1 h until the AsH₃ removal efficiency was below 95 % which was set as the "breakthrough point" of adsorbent. Adsorption capacity of the samples for AsH₃ was calculated as follows (Ning et al. 2011; Wang et al. 2014).

$$q = \frac{QC_0 t - Q \int_0^t C(t)dt}{m} \tag{1}$$

where $q$ is the adsorption capacity of the adsorbent (mg/g), $Q$ is the model gas flow rate (m³/min), $t$ is the adsorption time (min), $C_0$ is the influent AsH₃ concentration (mg/m³), $C(t)$ is the effluent AsH₃ concentration (mg/m³) at time $t$ (min), $m$ is the mass of adsorbent (g).

### 2.3 N₂ adsorption/desorption

The physical characteristics of the Co/Cu/AC adsorbents before and after AsH₃ adsorption, including the BET surface area, total pore volume, micropore volume, and average pore radius were measured with multi-spot nitrogen adsorption meter (NOVA 2000e, Quantachrome, USA).

## 3 Results and discussions

### 3.1 Effects of modifiers for AsH₃ removal

AsH₃ removal efficiency curves for different kinds of AC are shown in Fig. 2. The Co/Cu/AC adsorbent obviously shows a significant improvement in AsH₃ removal than other three adsorbents. When the adsorption time reached 4 h, the removal efficiency for Co/Cu/AC adsorbent was maintained at the goal of over 98 %. To achieve the effluent AsH₃ concentration of 15 mg/m³, there is a very long breakthrough time of about 17 h. According to the AsH₃ removal efficiency curves, the breakthrough adsorption capacities for AC, Co/AC, Cu/AC, and Co/Cu/AC are 8.7, 10.5, 15.8, and 29.8 mg/g, respectively. The excellent adsorption performance of Co/Cu/AC adsorbent may be due to the active groups formed after the introduction of CoPcS and Cu(NO₃)₂ (Wang et al. 2012).

**Fig. 1** Schematic diagram of the experiment (*1*) cylinder with O₂; (*2*) cylinder with AsH₃ (300 mg/m³ AsH₃ in N₂); (*3*) gas pressure reducer; (*4*) rotameter; (*5*) mixer; (*6*) three-way valve; (*7*) stop valve; (*8*) preheating implement; (*9*) adsorption column; (*10*) constant temperature water box; (*11*) AsH₃ tail gas absorber; (*12*) outlet sample point; (*13*) inlet sample point
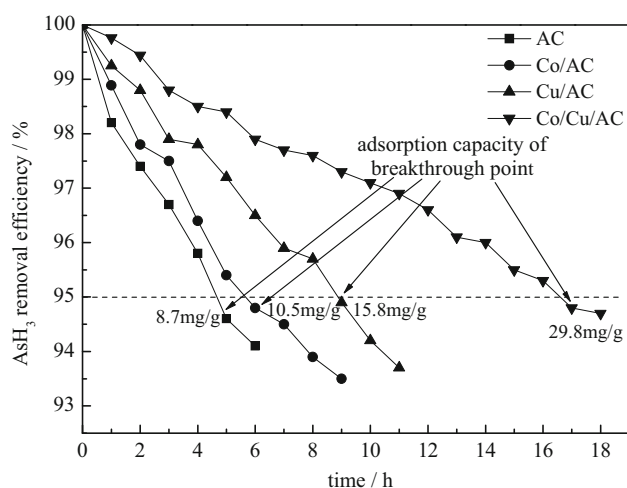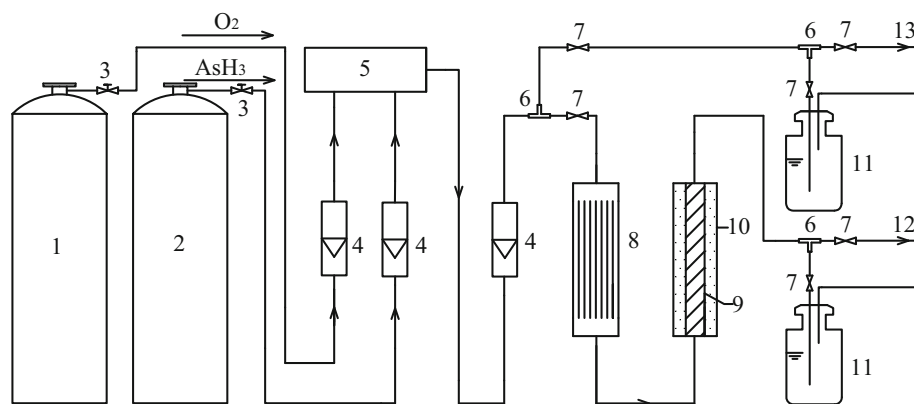
**Fig. 2** AsH₃ adsorption removal curves of different adsorbents. Experimental conditions: concentration of anhydrous methanol CoPcS solution = 0.04 %, concentration of aqueous Cu(NO₃)₂ solution = 0.2 mol/L, adsorbent amount = 2 g, T1 (calcination temperature) = 300 °C, T2 (adsorption temperature) = 60 °C, O₂ concentration = 1 %

**Fig. 3** Effects of CoPcS content on Co/Cu/AC adsorbents for AsH₃ adsorption. Experimental conditions: concentration of aqueous Cu(NO₃)₂ solution = 0.2 mol/L, adsorbent amount = 2 g, T1 (calcination temperature) = 300 °C, T2 (adsorption temperature) = 60 °C, O₂ concentration = 1 %

Therefore, the Co/Cu/AC adsorbent was selected for all subsequent experiments.

### 3.2 Effects of CoPcS content

The effects of CoPcS content on the Co/Cu/AC adsorbents for AsH₃ adsorption removal are shown in Fig. 3. According to the adsorption experimental results, the CoPcS content plays an important role for efficiently removing AsH₃. Figure 3 shows that the AsH₃ removal efficiency is enhanced with decreasing the CoPcS content. However, when the CoPcS content reaches a certain value (0.02 wt%), the enhancement of AsH₃ removal efficiency are not obvious. The maximum breakthrough adsorption capacity is 33.4 mg/g at CoPcS content of 0.02 wt%. According to theory of monolayer dispersion (Xie and Tang 1990; Wang et al. 2003), numerous salts and oxides
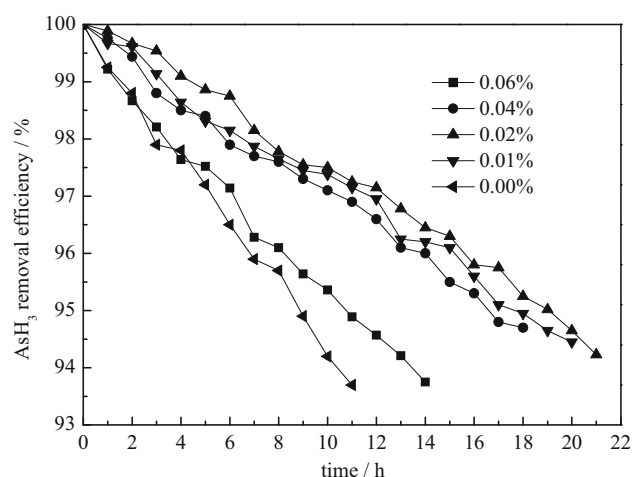
(include CoPcS) can be dispersed spontaneously on surfaces of supports to form a thermodynamically stable monolayer. When the CoPcS content is less than the dispersion capacity of AC support, the adsorption activity of AC adsorbents can be decreased. But if the CoPcS content is too high, the CoPcS molecules would aggregate with each other and produced many kinds of dimmers (Alcaraz et al. 1998; Jiang et al. 2001; Mei et al. 2007) leading to the decreased dispersion of CoPcS. The optimum CoPcS content is 0.02 wt% for Co/Cu/AC adsorbent.

### 3.3 Effects of calcination temperature

Generally, Cu(NO₃)₂·3H₂O is one of the most common precursors for preparing various adsorbents and catalysts, thus, the calcination temperature in the Co/Cu/AC adsorbent preparation processes is one of the most important factors influencing the AsH₃ removal efficiency and adsorption

capacity. Morozov et al. (2003) stated that the $Cu(NO_3)_2 \cdot 3H_2O$ formed $\beta$-$Cu_2(OH)_3NO_3$ from 199 °C to 217 °C at atmosphere pressure, while above 263 °C CuO was the final product. However, Tseng et al. (2003) indicated that the $Cu(NO_3)_2 \cdot 3H_2O$ decomposed to form CuO at 350 °C and CuO was well dispersed on surface of AC support. This suggested that CuO may be the major species on the Co/Cu/AC adsorbent for removing $AsH_3$. $AsH_3$ removal efficiency curves for Co/Cu/AC respectively calcined at 300, 350, 400, 450, 500 °C are presented in Fig. 4. According to the $AsH_3$ removal efficiency curves, when the calcination temperature is below 400 °C, the $AsH_3$ removal efficiency enhances with the increased temperature. But when the calcination temperature increases from 400 to 500 °C, the $AsH_3$ removal efficiency decreases greatly with the increased temperature and the $AsH_3$ breakthrough adsorption capacity decreases from 35.2 mg/g to 12.3 mg/g. Increasing the calcination temperature lead to accelerating AC support thermal decomposition. Furthermore, when the calcination temperature is above 450 °C, CuO and $Cu_2O$ could be formed simultaneously (Tseng et al. 2003; Yu et al. 2012). In addition, it is well known in literature that cobalt phthalocyanine derivatives are thermally stable up to 450 °C (Shen 2000). Singh et al. (2014) suggested that the CoPcS@ASMNP (nanosized silica coated magnetic nanoparticles immobilized CoPcS) catalyst was decomposed between 250–500 °C. Ebrahimian et al. (2014) indicated that the CoPcS was decomposed at 500 °C in CoPcS/$TiO_2$ catalyst because of the strong interaction between CoPcS and $TiO_2$. Based on the above analysis, 400 °C was selected as the optimal calcination temperature in the Co/Cu/AC adsorbent preparation processes.
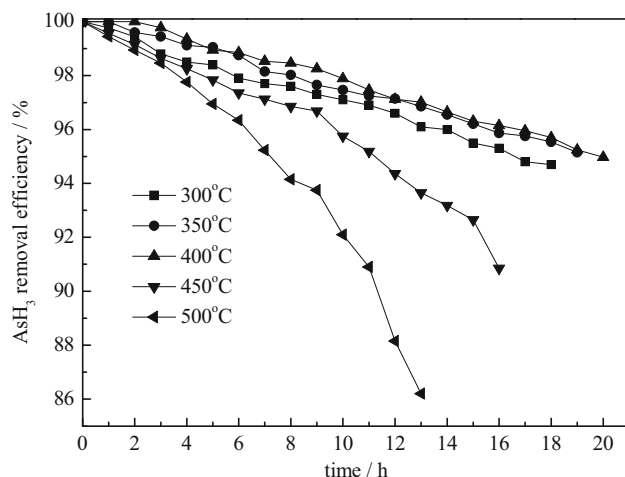
### 3.4 Effects of oxygen content

In our previous work, it was found that the adsorption processes of some highly toxic gases (such as $PH_3$, COS, HCN) on modified activated carbon (MAC) could be improved significantly by supplying micro-oxygen (Ning et al. 2011; Wang et al. 2011a, 2012, 2014; Jiang et al. 2012, 2013). The mechanism may be the adsorption (physical and chemical adsorption) and oxidation processes. Thus, the supplement of oxygen is also one of the most important factors influencing the $AsH_3$ removal efficiency. Figure 5 shows that the removal efficiency for $AsH_3$ in the model gas stream is significantly influenced by the $O_2$ concentration. In the absence of $O_2$, adsorption breakthrough of $AsH_3$ occurs in approximately 10 h and the $AsH_3$ removal efficiency decreases to 92.1 % at 16 h. As oxygen is introduced into the model gas stream, the prolonged breakthrough time of $AsH_3$ is observed. According to Fig. 5, the $AsH_3$ removal efficiency enhances with the increased oxygen content. With the oxygen content increases from 0 to 4 %, the $AsH_3$ breakthrough adsorption capacity increases from 17.6 to 36.9 mg/g. This result indicated that the oxygen in the model gas may take part in the $AsH_3$ removal process.

### 3.5 Effects on pore structure

Structural parameters of the Co/Cu/AC (before $AsH_3$ adsorption) and the Co/Cu/AC-$AsH_3$ (after $AsH_3$ adsorption) adsorbents are shown in Table 1. For the Co/Cu/AC-$AsH_3$ sample, the adsorption of $AsH_3$ resulted in the decrease of each textural property. The surface area, total

**Fig. 4** Effects of calcination temperature on Co/Cu/AC adsorbents for $AsH_3$ adsorption. Experimental conditions: concentration of anhydrous methanol CoPcS solution = 0.04 %, concentration of aqueous $Cu(NO_3)_2$ solution = 0.2 mol/L, adsorbent amount = 2 g, T2 (adsorption temperature) = 60 °C, $O_2$ concentration = 1 %
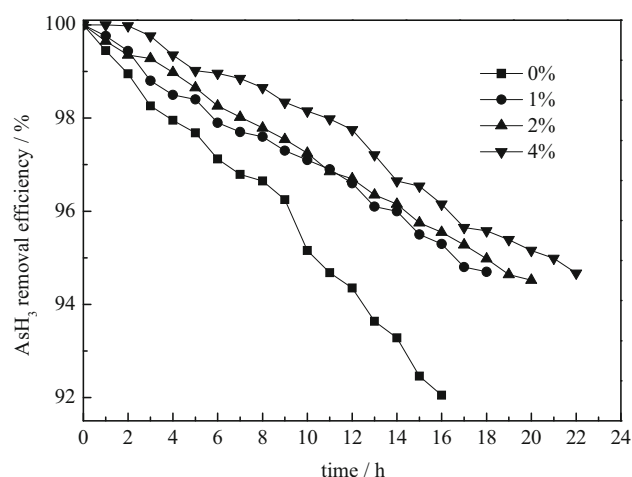
**Fig. 5** Effects of oxygen content on Co/Cu/AC adsorbents for $AsH_3$ adsorption. Experimental conditions: concentration of anhydrous methanol CoPcS solution = 0.04 %, concentration of aqueous $Cu(NO_3)_2$ solution = 0.2 mol/L, T1 (calcination temperature) = 300 °C, T2 (adsorption temperature) = 60 °C

**Table 1** Structure parameters of Co/Cu/AC adsorbents before and after AsH₃ adsorption

| Samples | BET surface area ($m^2 \, g^{-1}$) | Total pore volume ($cm^3 \, g^{-1}$) | Micropore volume ($cm^3 \, g^{-1}$) | Average pore radius (Å) |
|---|---|---|---|---|
| Co/Cu/AC | 849.6 | 0.4949 | 0.444 | 11.65 |
| Co/Cu/AC-AsH₃ | 797.5 | 0.4619 | 0.419 | 11.31 |
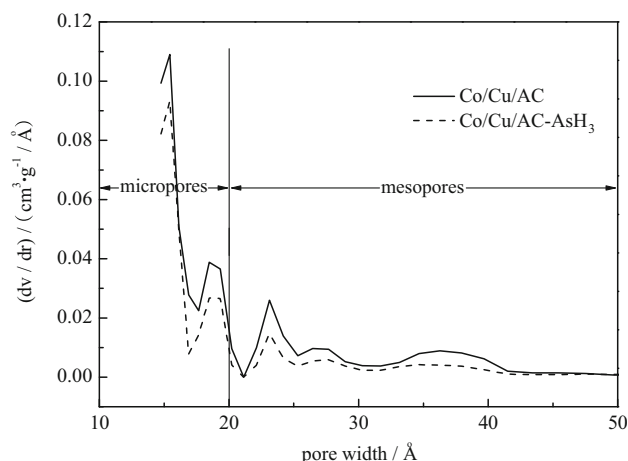


**Fig. 6** Comparison of pore size distributions of Co/Cu/AC adsorbents before and after AsH₃ adsorption



**Fig. 7** Effects of regeneration times for adsorbent regeneration performance

pore volume and micropore volume decrease by 6.1, 6.7 and 5.6 %, respectively. These results indicate that the pore structure of the Co/Cu/AC is influenced significantly by the AsH₃ adsorption process. The density functional theory (Ross and Olivier 1964) was used to calculate the Co/Cu/AC and Co/Cu/AC-AsH₃ pore size distributions which are showed in Fig. 6. The similar pore size distributions are observed before and after AsH₃ adsorption, except for the subtle change in the contributions of both micropores and mesopores to the total pore volumes. The most noticeable change is that the pore volume of Co/Cu/AC-AsH₃ decreased comparing with Co/Cu/AC in two sizes ranges of between 14.7 and 20 Å and between 20 and 43.4 Å. The micropores of AC adsorbents are favorable for AsH₃ physisorption which could be attributed to the small molecule structure of AsH₃ (Yu et al. 2000; Sekkat et al. 1995) and enhancement of adsorption potential (Bandosz 1999). Nevertheless, chemical processes may play an important role for AsH₃ adsorption/oxidation, and it may also occur in the micropores and mesopores.

### 3.6 Adsorbent regeneration

For regeneration, the Co/Cu/AC-AsH₃ sample was first reactivated by hot air for 3 h, then washed by hot water steam for 12 h. The aim of the water steam purging step was to remove the impurities (included the impurities on the surface of AC and the adsorption products after the
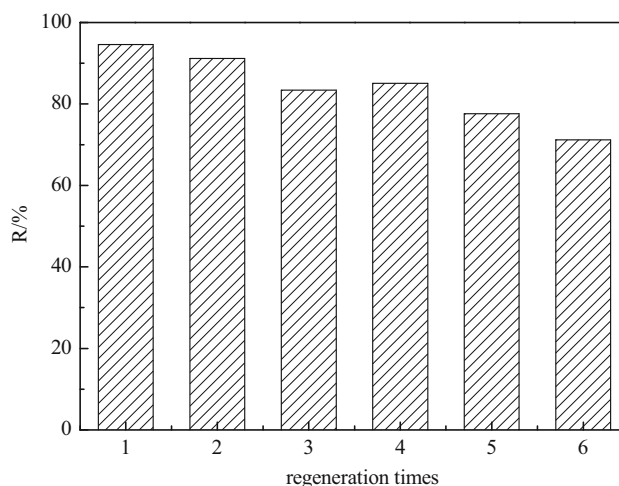
adsorption of AsH₃) of the Co/Cu/AC-AsH₃ adsorbent. The last step was sample drying at 110 °C for 24 h. The regeneration efficiency of R (R is the ratio of the breakthrough time of the regenerated adsorbent and fresh adsorbent) and the regeneration times were two key parameters for adsorbent regeneration performance. The effects of regeneration times for adsorbent regeneration performance are shown in Fig. 7. Obviously, the regeneration efficiency R was still as high as 71.2 % after six regeneration cycles for AsH₃. The average regeneration efficiency R was higher than 83.9 % indicating that the regeneration process was effective and the Co/Cu/AC adsorbent can be recycled.

### 4 Conclusions

(1) Three kinds of impregnated activated carbon adsorbents are prepared for removing low concentration AsH₃. The activity follows the order of Co/Cu/AC > Cu/AC > Co/AC. The AsH₃ breakthrough adsorption capacity for Co/Cu/AC is 3.4 times higher than unmodified AC.

(2) The CoPcS content, calcination temperature and oxygen content play important roles in the AsH₃ removal by Co/Cu/AC. The suitable conditions for the AsH₃ removal are CoPcS content of 0.02 wt%,

calcination temperature of 400 °C and oxygen content of 4 %

(3) The pore structure of adsorbents greatly affect the adsorption of AsH$_3$. The comparison of Co/Cu/AC samples before and after AsH$_3$ adsorption showed obvious differences in below 43.4 Å of pore width, especially in the range of 14.7–43.4 Å.

(4) The procedure of adsorbent regeneration is feasible and the regeneration efficiency maintains over 71.2 % after several regenerations.

# References

Alcaraz, J.J., Arena, B.J., Gillespie, R.D., Holmgren, J.S.: Solid base catalysts for mercaptan oxidation. Catal. Today **43**(1–2), 89–99 (1998)

Bandosz, T.J.: Effect of pore structure and surface chemistry of virgin activated carbons on removal of hydrogen sulfide. Carbon **37**(3), 483–491 (1999)

Cossel, K.C., Adler, F., Bertness, K.A., Thorpe, M.J., Feng, J., Raynor, M.W., Ye, J.: Analysis of trace impurities in semiconductor gas via cavity-enhanced direct frequency comb spectroscopy. Appl. Phys. B **100**(4), 917–924 (2010)

Ebrahimian, A., Zanjanchi, M.A., Noei, H., Arvand, M., Wang, Y.: TiO$_2$ nanoparticales containing sulphonated cobalt phthalocyanine: preparation, characterization and photocatalytic performance. J. Environ. Chem. Eng. **2**(1), 484–494 (2014)

Goldman, M., Dacre, J.C.: Lewisite: Its Chemistry, Toxicology, and Biological Effects. Springer, New York (1989)

Han, C.X., Han, X.Y., Li, Y., Liu, S.X., Zhang, B.G.: Removal of arsine in PH$_3$ by Fe-based alloy. Chin. J. Eng. Environ. **4**(7), 1601–1604 (2010)

Hidaka, K., Asahi, H., Yamamoto, K., Asami, K., Satoh, J., Gonda, S.: MOMBE growth of InGaAs using trisdimethylaminoarsenic. J. Cryst. Growth **181**(3), 193–196 (1997)

Howard, C.J., Dagle, R.A., Lebarbier, V.M., Rainbolt, J.E., Li, L.Y., King, D.L.: Progress toward biomass and coal-derived syngas warm cleanup: proof-of-concept process demonstration of multicontaminant removal for biomass application. Ind. Eng. Chem. Res. **52**(24), 8125–8138 (2013)

Ivandini, T.A., Yamada, D., Watanabe, T., Matsuura, H., Nakano, N., Fujishima, A., Einaga, Y.: Development of amperometric arsine gas sensor using gold-modified diamond electrodes. J. Electroanal. Chem. **645**(1), 58–63 (2010)

Jiang, D.E., Zhao, B.Y., Xie, Y.C., Pan, G.C., Ran, G.P., Min, E.Z.: Structure and basicity of γ-Al$_2$O$_3$-supported MgO and its application to mercaptan oxidation. Appl. Catal. A **219**(1–2), 69–78 (2001)

Jiang, M., Ning, P., Wang, Z.H., Xu, H.D., Miao, R.R., Wang, L.: Adsorption purification of low-concentration PH$_3$ by modified activated carbon. J. Chem. Eng. Chin. Univ. **26**(4), 685–691 (2012)

Jiang, M., Ning, P., Wang, Z.H., Xu, H.D., Zhou, J., Qin, Y.S.: Isothermal adsorption of H$_2$S and PH$_3$ on modified molecular sieve in oxygen-free or micro-oxygen ambience. J. Cent. South Univ. Sci. Technol. **44**(2), 854–861 (2013). In Chinese

Kawano, J., Kangawa, Y., Ito, T., Kakimoto, K., Koukitu, A.: Thermodynamic analysis of vapor-phase epitaxial growth of GaAsN on Ge. J. Cryst. Growth **343**(1), 105–109 (2012)

Mei, H., Hu, M., Ma, H.X., Yao, H.Q., Shen, J.: Preparation and characterization of NiO/MgO/Al$_2$O$_3$ supported CoPcS catalyst and its application to mercaptan oxidation. Fuel Process. Technol. **88**(4), 343–348 (2007)

Morozov, I.V., Znamenkov, K.O., Korenev, Y.M., Shlyakhtin, O.A.: Thermal decomposition of Cu(NO$_3$)$_2$·3H$_2$O at reduced pressures. Thermochim. Acta **403**(2), 173–179 (2003)

Ning, P., Wang, X.Y., Bart, H.J., Tian, S.L., Zhang, Y., Wang, X.Q.: Removal of phosphorus and sulfur from yellow phosphorus off-gas by metal-modified activated carbon. J. Clean. Prod. **19**(13), 1547–1552 (2011)

Ohno, T., Oyama, Y., Suto, K., Nishizawa, J.I.: Effects of AsH$_3$ surface treatment for the improvement of ultra-shallow area-selective regrown GaAs sidewall tunnel junction. Mater. Sci. Semicond. Process. **6**(5–6), 417–420 (2003a)

Ohno, T., Oyama, Y., Suto, K., Nishizawa, J.I.: Effect of surface stoichiometry on Be doping in GaAs by intermittent supply of AsH$_3$ and TEG in an ultra-high vacuum. Mater. Sci. Semicond. Process. **6**(5–6), 421–424 (2003b)

Oyama, Y., Ohno, T., Suto, K., Nishizawa, J.I.: Be doping in GaAs by intermittent AsH$_3$/TEG supply in an ultra-high vacuum. J. Cryst. Growth **259**(1–2), 61–68 (2003)

Oyama, Y., Nishizawa, J.I., Seo, K., Suto, K.: X-ray multi-crystal diffractometry analysis of heavily Te-doped GaAs grown by intermittent injection of TEGa/AsH$_3$ in ultra high vacuum. J. Cryst. Growth **213**(3–4), 221–228 (2000)

Quinn, R., Dahl, T.A., Diamond, B.W., Toseland, B.A.: Removal of arsine from synthesis gas using a copper on carbon adsorbent. Ind. Eng. Chem. Res. **45**(18), 6272–6278 (2006)

Quinn, R., Toseland, B.A.: Liquid-phase guard bed for removal of synthesis gas contaminants. Ind. Eng. Chem. Res. **47**(18), 7027–7030 (2008)

Ross, S., Olivier, J.P.: On Physical Adsorption. Interscience Publishers Wiley, New York (1964)

Rupp, E.C., Granite, E.J., Stanko, D.C.: Laboratory scale studies of Pd/γ-Al$_2$O$_3$ sorbents for the removal of trace contaminants from coal-derived fuel gas at elevated temperatures. Fuel **108**, 131–136 (2013)

Sekkat, Z., Komiha, N., Chraibi, M.: A representation of effective potentials of molecular fragments (NH$_3$, PH$_3$, AsH$_3$): applications to AH$_3$ - EH$_3$ systems, where A is B, Al, Ga, In or Tl, and E is N, P or As. J. Mol. Struct. **358**(1), 219–228 (1995)

Shen, Y.J.: The Syntheses and Applications of Phthalocyanines. Chemical Industry Press, Beijing (2000)

Singh, G., Khatri, P.K., Ganguly, S.K., Jain, S.L.: Magnetic silica beads functionalized with cobalt phthalocyanine for the oxidation of mercaptans in an alkali free aqueous medium. RSC Adv. **4**(55), 29124–29130 (2014)

Suh, J.K., Kang, N., Lee, J.B.: Direct determination of arsine in gases by inductively coupled plasma–dynamic reaction cell–mass spectrometry. Talanta **78**(1), 321–325 (2009)

Trembly, J.P., Gemmen, R.S., Bayless, D.J.: The effect of coal syngas containing AsH$_3$ on the performance of SOFCs: Investigations into the effect of operational temperature, current density and AsH$_3$ concentration. J. Power Sources **171**(2), 818–825 (2007)

Tseng, H.H., Wey, M.Y., Fu, C.H.: Carbon materials as catalyst support for SO$_2$ oxidation: catalytic activity of CuO-AC. Carbon **41**(1), 139–149 (2003)

Wang, C.M., Zhao, B.Y., Xie, Y.C.: Advances in the studies of spontaneous monolayer dispersion of oxides and salts on supports. Chin. J. Catal. **24**(6), 475–482 (2003)

Wang, X.Q., Ma, Y.X., Ning, P., Qiu, J., Ren, X.G., Li, Z.Y., Chen, W., Liu, W.: Adsorption of carbonyl sulfide on modified

activated carbon under low-oxygen content condition. Adsorption **20**(4), 623–630 (2014)

Wang, X.Q., Qiu, J., Ning, P., Ren, X.G., Li, Z.Y., Yin, Z.F., Chen, W., Liu, W.: Adsorption/desorption of low concentration of carbonyl sulfide by impregnated activated carbon under micro-oxygen conditions. J. Hazard. Mater. **229–230**, 128–136 (2012)

Wang, X.Q., Ning, P., Chen, W.: Studies on purification of yellow phosphorus off-gas by combined washing, catalytic oxidation, and desulphurization at a pilot scale. Sep. Purif. Technol. **80**(3), 519–525 (2011a)

Wang, Z.H., Jiang, M., Ning, P., Xie, G.: Thermodynamic modeling and gaseous pollution prediction of the yellow phosphorus production. Ind. Eng. Chem. Res. **50**(21), 12194–12202 (2011b)

Xie, Y.C., Tang, Y.Q.: Spontaneous monolayer dispersion of oxides and salts onto surfaces of supports: applications to heterogeneous catalysis. Adv. Catal. **37**, 1–43 (1990)

Yang, B.L., Cheung, N.W., Denholm, S., Shao, J., Wong, H., Lai, P.T., Cheng, Y.C.: Ultra-shallow n+p junction formed by $PH_3$ and $AsH_3$ plasma immersion ion implantation. Microelectron. Reliab. **42**(12), 1985–1989 (2002)

Yuan, X., Tian, S.L., Jiang, M., Zhou, J., Liu, Z.: Determination of total gaseous arsenic in yellow phosphorus tail gas using atomic fluorescence spectrometry. Chin. J. Anal. Lab. **33**(7), 774–777 (2014)

Yu, Q.F., Ning, P., Yi, H.H., Tang, X.L., Li, M., Yang, L.P.: Effect of preparation conditions on the property Cu/AC adsorbents for phosphine adsorption. Sep. Sci. Technol. **47**(3), 527–533 (2012)

Yu, X., Li, S.M., Liu, J.Y., Xu, Z.F., Li, Z.S., Sun, C.C.: Direct ab initio dynamics studies of the hydrogen abstraction reaction: $AsH_3+H \rightarrow AsH_2+H_2$. Chem. Phys. Lett. **320**(1–2), 123–128 (2000)